



## Minireview

## Development of radioligands with optimized imaging properties for quantification of nicotinic acetylcholine receptors by positron emission tomography

Andrew G. Horti<sup>\*</sup>, Yongjun Gao, Hiroto Kuwabara, Robert F. Dannals

Division of Nuclear Medicine, Department of Radiology, Johns Hopkins University, Baltimore, Maryland, United States

## ARTICLE INFO

## Article history:

Received 1 October 2008

Accepted 12 February 2009

## Keywords:

PET

Positron emission tomography

nAChR

Radioligand

Nicotine

Nicotinic acetylcholine receptor

## ABSTRACT

**Aims:** There is an urgent need for positron emission tomography (PET) imaging of the nicotinic acetylcholine receptors (nAChR) to study the role of the nicotinic system in Alzheimer's and Parkinson's diseases, schizophrenia, drug dependence and many other disorders. Greater understanding of the underlying mechanisms of the nicotinic system could direct the development of medications to treat these disorders. Central nAChRs also contribute to a variety of brain functions, including cognition, behavior and memory.

**Main methods:** Currently, only two radiotracers, (S)-3-(azetidin-2-ylmethoxy)-2-[<sup>18</sup>F]fluoropyridine (2-[<sup>18</sup>F]FA) and (S)-5-(azetidin-2-ylmethoxy)-2-[<sup>18</sup>F]fluoropyridine (6-[<sup>18</sup>F]FA), are available for studying nAChRs in human brain using PET. However, the "slow" brain kinetics of these radiotracers hamper mathematical modeling and reliable measurement of kinetic parameters since it takes 4–7 h of PET scanning for the tracers to reach steady state. The imaging drawbacks of the presently available nAChR radioligands have initiated the development of radioligands with faster brain kinetics by several research groups.

**Key findings:** This minireview attempts to survey the important achievements of several research groups in the discovery of PET nicotinic radioligands reached recently. Specifically, this article reviews papers published from 2006 through 2008 describing the development of fifteen new nAChR <sup>11</sup>C- and <sup>18</sup>F-ligands that show improved imaging properties over 2-[<sup>18</sup>F]FA.

**Significance:** The continuous efforts of radiomedical chemists led to the development of several interesting PET radioligands for imaging of nAChR including [<sup>18</sup>F]AZAN, a potentially superior alternative to 2-[<sup>18</sup>F]FA.

© 2009 Elsevier Inc. All rights reserved.

## Contents

Introduction	576
Currently available PET radioligands for imaging of nAChR in humans	576
Novel nAChR PET radioligands (2006–2008)	577
(±)-[ <sup>11</sup> C]NMI-EPB	577
[ <sup>18</sup> F]Nifene	578
(S)-3-(6-[ <sup>18</sup> F]fluorohex-1-ynyl)-5-((1-methylpyrrolidin-2-yl)methoxy)pyridine	578
[ <sup>11</sup> C]p-PVP-MEMA	578
[ <sup>11</sup> C]JHU85208, [ <sup>11</sup> C]JHU85157 and [ <sup>11</sup> C]JHU85270	578
[ <sup>18</sup> F]FPhEP and [ <sup>18</sup> F]F2PhEP	579
[ <sup>18</sup> F](-)-NCFHEB	579
[ <sup>18</sup> F]AZAN ([ <sup>18</sup> F]JHU87522) and its analogs	580
Further preclinical studies with [ <sup>18</sup> F](-)-JHU87522 ([ <sup>18</sup> F]AZAN)	581
Metabolism studies in mice and baboon	581
nAChR-subtype inhibition binding assay	581
In vitro functional assay of [ <sup>18</sup> F](-)-JHU87522 ([ <sup>18</sup> F]AZAN)	581
Preliminary safety studies with [ <sup>18</sup> F](-)-JHU87522 ([ <sup>18</sup> F]AZAN)	581
Synthesis of [ <sup>18</sup> F](-)-JHU87522 ([ <sup>18</sup> F]AZAN)	582

<sup>\*</sup> Corresponding author. PET Center, Division of Nuclear Medicine, Radiology, Johns Hopkins Medicine, 600 North Wolfe Street, Nelson B1-122, Baltimore, MD 21287-0816, United States. Tel.: +1 410 614 5130.

E-mail address: [ahorti1@jhmi.edu](mailto:ahorti1@jhmi.edu) (A.G. Horti).

Conclusion . . . . .	582
Acknowledgements . . . . .	582
References . . . . .	582

## Introduction

The  $\alpha 4\beta 2$ -subtype of the nicotinic acetylcholine receptors (nAChR) is the most prominent subtype of nicotinic acetylcholine receptors in mammalian brain with highest density of the receptor in thalamus, intermediate density in cortical regions and caudate and lowest in cerebellum (Lukas et al. 1999; Pimlott et al. 2004).  $\alpha 4\beta 2$ -nAChR is relevant to various brain functions including cognition, memory and behavior. There is strong evidence of the role of  $\alpha 4\beta 2$ -nAChRs and alteration of density of the receptor in central nervous system (CNS) disorders, such as Alzheimer's disease, Parkinson's disease, schizophrenia, depression, attention deficit hyperactivity disorder (ADHD) and tobacco dependence (Holladay et al. 1997; Paterson and Nordberg 2000; Pimlott et al. 2004). The approximate lifetime prevalence of Alzheimer's is 1.5%, schizophrenia – 1%, Parkinson's – 0.15%, and ADHD – 5.3% in people under the age of 19. Approximately 1.1 billion people worldwide smoke and risk the addictive potential of tobacco and its harmful effects. Even though structure, pharmacology and biochemistry of nAChR have been studied for many years the involvement of the receptor in human physiology remains elusive (Gotti et al. 1997). Better understanding of the principal mechanisms of the nAChR in CNS could facilitate the development of nicotinic-specific drugs to treat many disorders (Gotti et al. 2006).

Currently, positron emission tomography (PET) is the most advanced modality for non-invasive study of cerebral receptors. PET studies display better resolution and accuracy in quantification of regional distribution and temporal measurements of radioactivity and thus are superior to all other imaging modalities including single photon emission computed tomography (SPECT) (Alavi and Basu 2008; Rahmim and Zaidi 2008). The limited availability of the PET radioligands for CNS receptor imaging justified the substantial efforts for development of novel PET radioligands.

To our knowledge, only three radiotracers, [ $^{11}\text{C}$ ]nicotine, (S)-3-(azetidin-2-ylmethoxy)-2- $^{18}\text{F}$ fluoropyridine (2- $^{18}\text{F}$ FA) and (S)-5-(azetidin-2-ylmethoxy)-2- $^{18}\text{F}$ fluoropyridine (6- $^{18}\text{F}$ FA) (Table 1), have been used for studying  $\alpha 4\beta 2$ -nAChRs in human brain using PET. The PET imaging properties of these radioligands are not perfect. Poor signal-to-noise ratios and other drawbacks of [ $^{11}\text{C}$ ]nicotine suggest that this radiotracer is not well suited for quantitative imaging in

animals and humans. The “slow” brain kinetics of 2- $^{18}\text{F}$ FA and 6- $^{18}\text{F}$ FA hamper mathematical modeling and reliable kinetic parameter estimation since it takes many hours of PET scanning (5–7 h) for the tracer radioactivity to reach a spatial-temporal steady state.

Despite the substantial drawbacks of 2- $^{18}\text{F}$ FA, this radioligand has been used in several recent PET studies (Mitkovski et al. 2005; Brody et al. 2006; Picard et al. 2006; Ellis et al. 2008; Kimes et al. 2008; Mukhin et al. 2008; Sabri et al. 2008) suggesting a high demand for nAChR PET radioligands. The latest publication (Ellis et al. 2008) reported the methodological limitations of the 2- $^{18}\text{F}$ FA PET highlighting the need for better nAChR PET radioligands. Therefore discovery of radioligands for  $\alpha 4\beta 2$ -nAChRs with better imaging properties than 2- $^{18}\text{F}$ FA and 6- $^{18}\text{F}$ FA is strongly awaited by the PET imaging community.

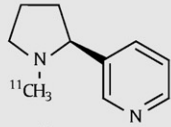
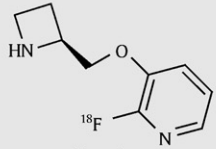
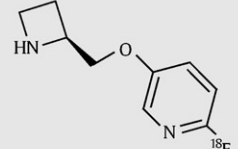
Previous reviews have described development of PET radioligands for imaging of nAChR radioligands and covered the literature that was published before 2006 (Villemagne et al. 1999; Gundisch 2000; Paterson and Nordberg 2000; Sihver et al. 2000a,b; Volkow et al. 2001; Ding and Fowler 2005; Horti and Villemagne 2006). This minireview surveys the 2006–2008 articles that describe progress in developing a PET radiotracer for imaging of nAChR with better brain kinetics than those of 2- $^{18}\text{F}$ FA and 6- $^{18}\text{F}$ FA.

## Currently available PET radioligands for imaging of nAChR in humans

[ $^{11}\text{C}$ ]Nicotine (Table 1) has been known for many years (Maziere et al. 1976) as a PET radioligand, but it has poor imaging properties in animals and humans due to high non-specific binding, low specific binding and rapid metabolism (see the reviews that are quoted in the previous paragraph).

2- $^{18}\text{F}$ FA and 6- $^{18}\text{F}$ FA are the currently available radioligands for quantitative imaging nAChR in humans. Unfortunately, both radioligands exhibit slow brain distribution kinetics and relatively low BP in monkey and human brain (Table 1) (Horti and Villemagne 2006). Quantitative PET studies require many hours for 2- $^{18}\text{F}$ FA and 6- $^{18}\text{F}$ FA to reach steady-state in the brain. Kinetic modeling of 2- $^{18}\text{F}$ FA in Rhesus monkey showed that at least 5 h of PET acquisition are necessary to estimate the total distribution volume (DV) with an error

**Table 1**  
A comparison of in vitro and in vivo parameters for nAChR radioligands available for clinical PET studies.

Radioligand			
Property	(-)-[ $^{11}\text{C}$ ]nicotine <sup>g</sup>	2- $^{18}\text{F}$ FA <sup>h</sup>	6- $^{18}\text{F}$ FA <sup>i</sup>
Inhibition binding affinity $K_i$ , nM ( $K_{rel}$ ) <sup>a</sup>	1 (40–60)	0.061 (6.1)	0.025 (2.2)
Partition coefficient $\log D_{7.4}$	0.02 <sup>b</sup>	-1.43 <sup>c</sup>	-1.9 <sup>b</sup>
Bolus injection peak uptake in Rhesus, min	5	~120	~120
Bolus injection peak uptake in human, min	3–5	~120	~120
BP <sup>Th</sup> or (Th/CB ratio) <sup>f</sup>	(1.1) <sup>d</sup>	2 <sup>d</sup>	3.5 <sup>e</sup> ; (4.2) <sup>d</sup>

<sup>a</sup>Precise inhibition assay conditions differ between laboratories. Therefore,  $K_{rel}$ , a ratio of the inhibition binding affinity ( $K_i$ ) for the test compound to that of (-)-epibatidine from the same laboratory and by the same method, provide a sense of comparative affinity; <sup>b</sup>Calculated by ACD/logD software; <sup>c</sup>Experimental  $\log D_{7.4}$ ; <sup>d</sup>Rhesus monkey; <sup>e</sup>DV ratio for thalamus/cerebellum in baboon; <sup>f</sup>Th = thalamus, CB = cerebellum; <sup>g</sup>(Maziere et al. 1976; Sullivan et al. 1996; Muzic et al. 1998; Sihver et al. 1999; Paterson and Nordberg 2000); <sup>h</sup>(Dolle et al. 1998; Horti et al. 1998a; Brown et al. 2002; Bottlaender et al. 2003; Chefer et al. 2003; Zhang et al. 2004); <sup>i</sup>(Ding et al. 2000; Horti et al. 2000; Ding et al. 2004; Gundisch et al. 2005).

<5%. More precise measurement of the total DV in thalamus required up to 7 h of scanning (Fig. 1) (Chefer et al. 2003). In baboons the peak uptake of 2-[ $^{18}$ F]FA in thalamus was at approximately 140 min post administration and the acquisition time was greater than 200 min for quantitative measurements (Valette et al. 1999). Although it has been shown that a two-hour scan duration might be sufficient for estimating BP in extrathalamus regions with 2-[ $^{18}$ F]FA (Mitkovski et al. 2005), BP estimates disagreed for thalamus among full-kinetics approaches and reference tissue methods as effects of not including steady-state data in the analysis varied on individual methods. Clinical PET studies with 6-[ $^{18}$ F]FA showed that at least 4 h scanning time is necessary whereas the BP values of this radioligand were slightly greater than those of 2-[ $^{18}$ F]FA (Ding et al. 2004). Despite the somewhat improved imaging properties of 6-[ $^{18}$ F]FA versus 2-[ $^{18}$ F]FA thus far only one publication has described the human PET experiments with 6-[ $^{18}$ F]FA (Ding et al. 2004). Perhaps, the limited number of human PET studies with 6-[ $^{18}$ F]FA is due to the concerns of the relatively high toxicity of this radioligand (Scheffel et al. 2000).

Another crucial problem with 2-[ $^{18}$ F]FA and 6-[ $^{18}$ F]FA is relatively low BP in extrathalamic regions ( $BP \leq 0.6$ – $0.8$ ), including cortex, which have lower densities of the receptor. The importance of imaging of extrathalamic nAChRs has emerged from the demonstration of altered densities of cortical and striatal nAChRs in neurodegenerative diseases (Pimlott et al. 2004) and schizophrenia (Ochoa and Lasalde-Dominicci 2007).

The slow brain kinetics of 2-[ $^{18}$ F]FA and 6-[ $^{18}$ F]FA are the main reason why these radiolabeled probes are used less widely than one would anticipate for such an important target as cerebral nAChRs. Few PET centers have the time and funding available for these lengthy procedures. The bolus-plus-infusion (B/I) scheme (Carson et al. 1993; Watabe et al. 2000) may be useful to overcome the slow brain kinetics of 2-[ $^{18}$ F]FA by shortening in-scan time to less than 1 h. However, a recent work (Kimes et al. 2008) indicated that it would require 6 h of continuous infusion for 2-[ $^{18}$ F]FA before starting the scan to reach a steady-state via the B/I method. Therefore, the B/I imaging method with 2-[ $^{18}$ F]FA appears to be impractical for routine use.

### Novel nAChR PET radioligands (2006–2008)

The imaging drawbacks of 2-[ $^{18}$ F]FA that were mentioned above have prompted the development of radioligands with faster brain kinetics by several research groups. Among the most interesting recent radioligands with rapid brain kinetics are ( $\pm$ )-[ $^{11}$ C]NMI-EPI

(Ding et al. 2006), [ $^{18}$ F]nifene (Pichika et al. 2006; Easwaramoorthy et al. 2007), [ $^{11}$ C]p-PVP-MEMA (Dolle et al. 2008), [ $^{18}$ F]FPhEP and [ $^{18}$ F]F2PhEP (Roger et al. 2006; Valette et al. 2007), [ $^{18}$ F](-)NCFHEB (Deuther-Conrad et al. 2004; Brust et al. 2008; Deuther-Conrad et al. 2008) and two JHU series (Gao et al. 2007a,b,c, 2008b). These will be discussed below.

### ( $\pm$ )-[ $^{11}$ C]NMI-EPB

The high affinity ( $K_i = 29$  pM) epibatidine analog, 7-methyl-2-exo-(3'-iodo-5'-pyridinyl)-7-azabicyclo[2.2.1]heptane (NMI-EPB), having weak agonist and potent antagonist activity (Carroll et al. 2005) was radiolabeled with  $^{11}$ C (Ding et al. 2006). The preliminary baseline and blocking experiments in baboon demonstrated high brain uptake ( $\sim 0.05\%$  injected dose/cc in thalamus), high signal-to-noise ratio (Thalamus/Cerebellum = 2.5–3.5), and high specific binding of [ $^{11}$ C]NMI-EPB (Fig. 2) (Ding et al. 2006). PET modeling analysis was not presented in the paper, but the authors suggested that [ $^{11}$ C]NMI-EPB exhibited relatively fast kinetics in the baboon brain ( $t_{1/2} = 60$ – $90$  min) and might achieve an equilibrium faster than 2-[ $^{18}$ F]FA and 6-[ $^{18}$ F]FA.

In a recent study (Gao et al. 2008a) enantiomers of ( $\pm$ )-NMI-EPB were separated by semi-preparative chiral HPLC. Inhibition binding assays of these enantiomers showed that (+)-NMI-EPB ( $K_i = 2310$ ;  $1680$  pM) exhibited binding affinity that was too low to be a good PET radioligand and only (-)-NMI-EPB ( $K_i = 55$ ;  $68$  pM) was suitable for PET imaging. The enantiomer (-)-NMI-EPB was radiolabeled with  $^{11}$ C and (-)-[ $^{11}$ C]NMI-EPB was injected into a baboon. (-)-[ $^{11}$ C]NMI-EPB showed good accumulation of radioactivity in the nAChR-rich thalamus and lower accumulation in nAChR-poor cerebellum. Yet the brain kinetics of (-)-[ $^{11}$ C]NMI-EPB were relatively slow (Fig. 3). There was a continuous increase of uptake in the baboon thalamus and decrease of radioactivity in the cerebellum during the 90 min of scanning suggesting that this scan duration was not sufficient for the radioligand to reach steady-state. Extension of the scanning time of (-)-[ $^{11}$ C]NMI-EPB beyond 90–120 min was not practical due to the short half-life of  $^{11}$ C. The paper (Gao et al. 2008a) concluded that the seemingly rapid brain kinetics of the racemic tracer ( $\pm$ )-[ $^{11}$ C]NMI-EPB (Ding et al. 2006) was a superimposition of two kinetics: the slow kinetics of the active enantiomer (-)-[ $^{11}$ C]NMI-EPB and rapid kinetics of non-specific binding of the inactive enantiomer (+)-[ $^{11}$ C]NMI-EPB. A recent publication (Gao et al. 2007a) has described such a superimposition of brain kinetics of active and inactive enantiomers

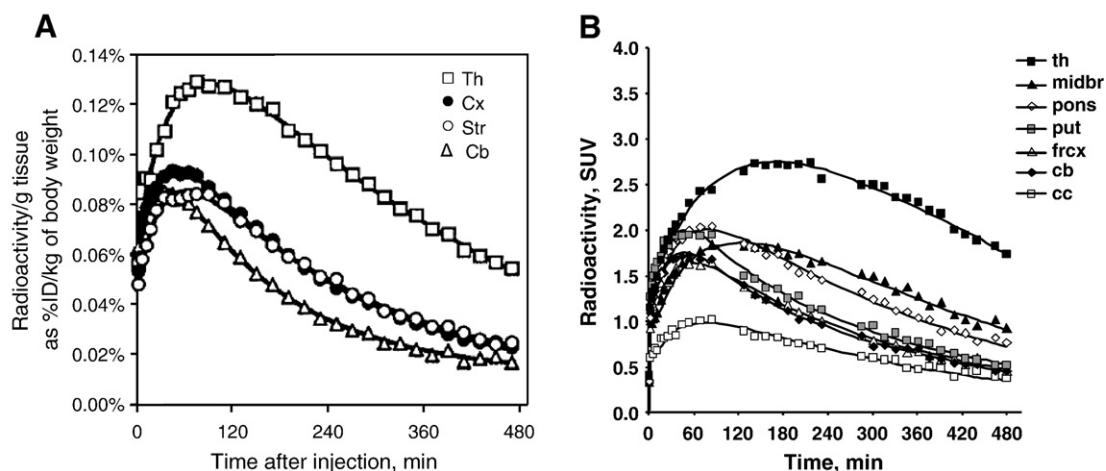


**Fig. 1.** A: Time-uptake curves of 2-[ $^{18}$ F]FA in various brain regions of the Rhesus monkey (reprinted from (Chefer et al. 2003) with permission of Wiley–Blackwell). Symbols: Cb = cerebellum, Th = thalamus, Cx = cortex, Str = striatum; B: Time-uptake curves of 2-[ $^{18}$ F]FA in the brain regions of the control human subjects (obtained from Dr. Alane Kimes of NIDA NIH). Symbols: cc = corpus callosum, frcx = frontal cortex, cb = cerebellum, midbr = mesencephalon, put = putamen, th = thalamus.

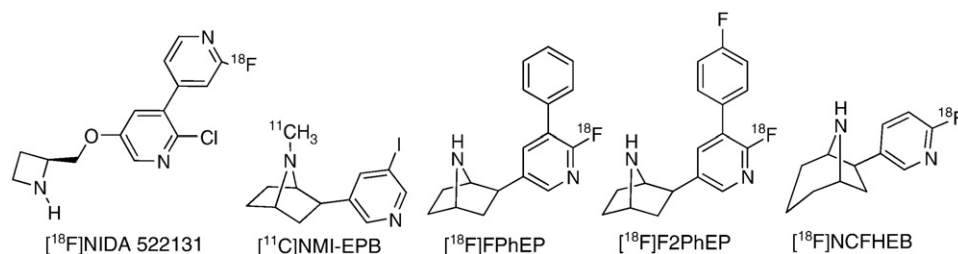


Fig. 2. Structures of  $[^{18}\text{F}]\text{NIDA } 522131$ ,  $[^{11}\text{C}]\text{NMI-EPB}$ ,  $[^{18}\text{F}]\text{FPhEP}$ ,  $[^{18}\text{F}]\text{F2PhEP}$  and  $[^{18}\text{F}]\text{NCFHEB}$ .

of radiolabeled analogs of NMI-EPI in baboons. The paper concluded that  $(-)-[^{11}\text{C}]\text{NMI-EPB}$ , the active enantiomer of the previously described  $(\pm)-[^{11}\text{C}]\text{NMI-EPB}$ , was not suitable for reliable mathematical PET modeling due to the slow brain kinetics (Gao et al. 2008a). We are not aware of detailed toxicological studies with  $(\pm)-\text{NMI-EPB}$  and  $(-)-\text{NMI-EPB}$ . Carroll et al. 2005 reported antinociception studies in mice when doses of 0.4–0.8 mg/kg (1250–2500 nmol/kg)  $(\pm)-\text{NMI-EPB}$  were injected subcutaneously (s.c.). In our unpublished studies intravenous injection of 0.06 mg/kg (190 nmol/kg)  $(\pm)-\text{NMI-EPB}$  produced the Straub tail in mice and reduced locomotor activity, but no death. These data demonstrate a relatively low adverse effect of NMI-EPB that is likely due to its functional properties as an nAChR antagonist (Carroll et al. 2005). The binding affinity value of NMI-EPB with ganglionic  $\alpha3\beta4$ -nAChR has not been published. Therefore, it is difficult to conclude if the nAChR-subtype selectivity also contributes to the moderate pharmacological adverse effects of NMI-EPB in mice.

### $[^{18}\text{F}]\text{Nifene}$

Targeting an agonist PET imaging agent for  $\alpha4\beta2$ -nAChR receptor with relatively rapid kinetics compared to 2- $[^{18}\text{F}]\text{FA}$ , the PET group at University of California–Irvine suggested that an analog of 2- $[^{18}\text{F}]\text{FA}$  with lower binding affinity might exhibit desired imaging properties (Pichika et al. 2006). The group synthesized an interesting nAChR radioligand,  $[^{18}\text{F}]\text{nifene}$  (Fig. 4) ( $K_i = 0.5$  nM;  $\log D_{7.4} = -0.52$ ), by nucleophilic fluorination of the corresponding N-BOC-nitro-precursor followed by deprotection with trifluoroacetic acid. PET studies in Rhesus monkey with  $[^{18}\text{F}]\text{nifene}$  showed rapid accumulation of radioactivity in the nAChR-rich thalamus with peak at 5 min post injection (0.02%ID/mL) and lower accumulation of the radioactivity in the nAChR-poor cerebellum. The thalamus/cerebellum ratio in the monkey brain reached the value of about 2.2 at 0.5 h post-injection

and this ratio decreased overtime after the peak. This highly reversible kinetics of  $[^{18}\text{F}]\text{nifene}$  in the monkey brain suggested that the radioligand has a potential for clinical studies (Pichika et al. 2006), but no human studies were reported since, perhaps, due to the relatively low target-to-non-target ratio of  $[^{18}\text{F}]\text{nifene}$ . However, the same group demonstrated usefulness of the radioligand in in vitro blocking studies with acetylcholine in presence of acetylcholinesterase inhibitors (Easwaramoorthy et al. 2007).

### (S)-3-(6- $[^{18}\text{F}]\text{fluorohex-1-ynyl}$ )-5-((1-methylpyrrolidin-2-yl)methoxy)pyridine

(S)-3-(6- $[^{18}\text{F}]\text{fluorohex-1-ynyl}$ )-5-((1-methylpyrrolidin-2-yl)methoxy)pyridine (Fig. 4) was synthesized as a highly selective  $\beta2$ -nAChR ligand ( $K_i^{\alpha4\beta2} = 0.95$  nM,  $K_i^{\alpha3\beta4} = 88000$  nM) (Wei et al. 2005). Radiolabeling of the ligand with  $^{11}\text{C}$  and  $^{18}\text{F}$  gave two isotopomers that were studied in baboon (Kozikowski et al. 2006). Both radioligands exhibited similar imaging properties with peak in thalamus at 3–4 min post-injection (2.5–3%ID/100 mL). The kinetics in all brain regions were highly reversible. Even though the PET modeling was not presented the time–uptake curves demonstrate that both radioligands probably reached steady-state within 60 min post injection. The thalamus/cerebellum ratio was about 2–2.5 at 60 min post injection. Unexpectedly, both radioligands exhibited uptake in the nAChR-poor striatum that was comparable with that in the nAChR-rich thalamus. Blocking studies with nicotine resulted in inhibition of uptake in thalamus (8%) and cerebellum (1%), whereas blockade in striatum was insignificant. The authors suggested that active metabolites could be responsible for the binding with striatum. No further studies have been published.

### $[^{11}\text{C}]\text{p-PVP-MEMA}$

(R,E)-1-(6-chloro-5-(2-(pyridin-4-yl)vinyl)pyridin-3-yloxy)-N-methylpropan-2-amine (Fig. 5), a nAChR ligand with  $K_i = 77$  pM (Lin et al. 2002), was chosen for radiolabeling with  $^{11}\text{C}$  (Dolle et al. 2008) because of the structural similarity of this compound to the previously developed  $[^{11}\text{C}]\text{Me-PVC}$  (Brown et al. 2002), a high affinity nAChR radioligand ( $K_i = 28$  pM) with rapid brain kinetics in the monkey brain (Brown et al. 2004). (R,E)-1-(6-chloro-5-(2-(pyridin-4-yl)vinyl)pyridin-3-yloxy)-N- $[^{11}\text{C}]\text{methylpropan-2-amine}$  ( $[^{11}\text{C}]\text{p-PVP-MEMA}$ ) was prepared by radiomethylation of the corresponding desmethyl precursor (Dolle et al. 2008). Dynamic PET studies in baboon showed that  $[^{11}\text{C}]\text{p-PVP-MEMA}$  entered the brain with maximal uptake value of 0.4–0.6%ID/100 mL at 2 min after injection. The regional brain distribution of the radioligand manifested little specific binding with thalamus/cerebellum ratio  $\sim 1$  at 1 h post injection. The paper concluded that a possible reason for the low signal-to-noise ratio was the poor metabolic stability of the parent compound.

### $[^{11}\text{C}]\text{JHU85208}$ , $[^{11}\text{C}]\text{JHU85157}$ and $[^{11}\text{C}]\text{JHU85270}$

With the goal of developing a nAChR radioligand with rapid brain kinetics and good binding potentials the Johns Hopkins group recently

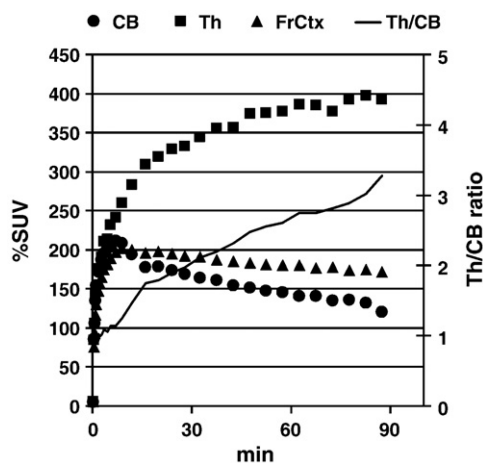


Fig. 3. Regional time-uptake curves of  $[^{11}\text{C}]\text{-NMI-EPB}$  in the baboon brain (Gao et al. 2008a). Symbols: CB = cerebellum, Th = thalamus, FrCtx = frontal cortex, Th/CB = thalamus/cerebellum ratio.



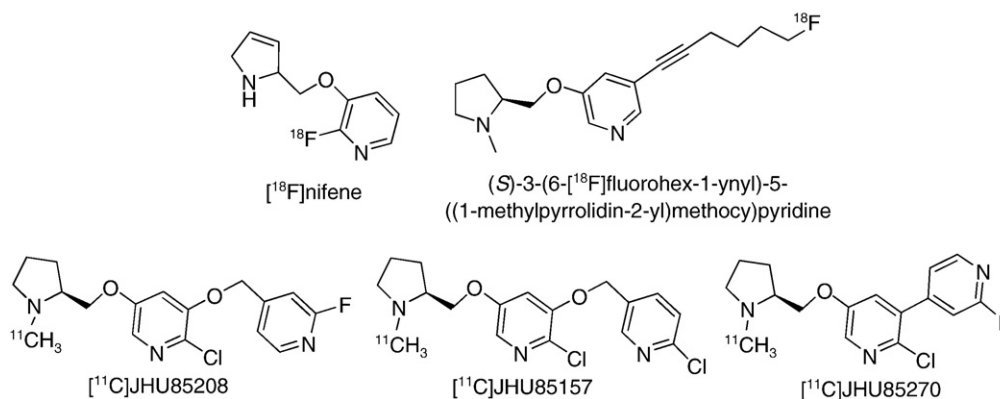


Fig. 4. New pyrrolidine-based nAChR PET radioligands.

synthesized [ $^{11}\text{C}$ ]JHU85208, [ $^{11}\text{C}$ ]JHU85157 and [ $^{11}\text{C}$ ]JHU85270 (Fig. 4) (Gao et al. 2007b,c), radiolabeled analogs of [ $^{11}\text{C}$ ]Me-PVC (Brown et al. 2002, 2004; Horti and Villemagne 2006). These  $^{11}\text{C}$ -pyrrolidine compounds demonstrated rapid uptake in baboon brain regions (Table 2) and all three reached steady-state in baboon thalamus within 120 min post-administration. Yet, the BP values of [ $^{11}\text{C}$ ]JHU85208, [ $^{11}\text{C}$ ]JHU85157 and [ $^{11}\text{C}$ ]JHU85270 were all below 1 and, thus, too low for quantitative PET studies (Table 2). The low BP values were unexpected by the group after taking into consideration the very high binding affinities of these radioligands. However, metabolite analyses of [ $^{18}\text{F}$ ]JHU85208, [ $^{18}\text{F}$ ]JHU85157 and [ $^{18}\text{F}$ ]JHU85270 demonstrated that all three radioligands rapidly metabolized to lipophilic radiolabeled compounds that were likely to penetrate the BBB (Gao et al. 2007b,c). Non-specific binding of these lipophilic metabolites were suggested to be a reason of the relatively high non-specific binding and low BP values of the radioligands.

#### [ $^{18}\text{F}$ ]FPhEP and [ $^{18}\text{F}$ ]F2PhEP

Two epibatidine-based antagonists of nAChR, 2-(6-fluoro-5-phenylpyridin-3-yl)-7-aza-bicyclo[2.2.1]heptane (FPhEP) and 2-(6-fluoro-5-(4-fluorophenyl)pyridin-3-yl)-7-aza-bicyclo[2.2.1]heptane (F2PhEP), with inhibition binding affinity values of  $K_i = 240$  pM and 29 pM, correspondingly, were developed as potential pharmacotherapies for treatment of smoking cessation (Carroll et al. 2004). Due to their excellent  $\alpha 4\beta 2$ -nAChR subtype selectivity (Huang et al. 2005) and functional properties as nAChR antagonists these compounds can be injected in mice s.c. at high doses of up to 15 mg/kg. The high binding affinity, low toxicity and suitability for radiolabeling with  $^{18}\text{F}$  attracted the attention of PET radiochemists to these ligands (Fig. 2) (Roger et al. 2006; Valette et al. 2007). Dynamic PET data (Valette et al. 2007) were acquired after injection of 215 MBq of [ $^{18}\text{F}$ ]FPhEP or [ $^{18}\text{F}$ ]F2PhEP in baboon.

[ $^{18}\text{F}$ ]FPhEP manifested rapid kinetics with thalamic radioactivity peaking at 20 min (4.9% ID/100 mL tissue), whereas [ $^{18}\text{F}$ ]F2PhEP, an analog of [ $^{18}\text{F}$ ]FPhEP with substantially greater binding affinity, showed peak in baboon thalamus at 45 min (3.3% ID/100 mL tissue). In the blocking studies nicotine, cytosine, or FPhEP reduced the brain

uptake of [ $^{18}\text{F}$ ]FPhEP. Unfortunately, the thalamus/cerebellum ratio of [ $^{18}\text{F}$ ]FPhEP (1.4 at 30 min postinjection) was low and did not increase with time suggesting that the radioligand is not suitable for quantitative PET studies. Baseline PET experiments with [ $^{18}\text{F}$ ]F2PhEP and blocking studies with nicotine demonstrated that the specific binding of this radioligand in vivo was low. The paper concluded that in spite of a moderate to high in vitro binding affinity, [ $^{18}\text{F}$ ]FPhEP or [ $^{18}\text{F}$ ]F2PhEP did not fulfill the widely adopted criteria for a PET radioligand. The authors suggested that high lipophilicities of [ $^{18}\text{F}$ ]FPhEP ( $\text{clogP} = 2.87$ ) or [ $^{18}\text{F}$ ]F2PhEP ( $\text{clogP} = 3.01$ ) were the cause of high non-specific binding of both compounds in the baboon brain.

#### [ $^{18}\text{F}$ ](-)-NCFHEB

Two enantiomers of 6-(6-[ $^{18}\text{F}$ ]fluoropyridin-3-yl)-8-aza-bicyclo[3.2.1]octane ([ $^{18}\text{F}$ ]NCFHEB) (Fig. 2), (-)-[ $^{18}\text{F}$ ]NCFHEB and (+)-NCFHEB, were developed by the PET group from Leipzig (Deuther-Conrad et al. 2004; Brust et al. 2008; Deuther-Conrad et al. 2008). The compounds are  $\alpha 4\beta 2$ -nAChR ligands with  $K_i$  values of 112 pM ((-)-NCFHEB) and 64 pM ((+)-NCFHEB). Inhibition binding affinity of both enantiomers with  $\alpha 3\beta 4$ -nAChR subtype was low suggesting their low toxicity (Deuther-Conrad et al. 2004). No pharmacological adverse effects were observed in mice when larger-than-tracer doses of (+)-NCFHEB and (-)-NCFHEB (25  $\mu\text{g/kg}$  or 120 nmol/kg) were injected intravenously. The functional properties of NCFHEB have not been reported.

In vivo (-)-[ $^{18}\text{F}$ ]NCFHEB or (+)-[ $^{18}\text{F}$ ]NCFHEB specifically labeled the cerebral nAChR in mice and exhibited a greater accumulation of radioactivity in the nAChR-rich brain regions than that of 2-[ $^{18}\text{F}$ ]FA (Deuther-Conrad et al. 2008). The in vivo brain kinetics of (+)-[ $^{18}\text{F}$ ]NCFHEB, (-)-[ $^{18}\text{F}$ ]NCFHEB and 2-[ $^{18}\text{F}$ ]FA were compared in pigs in baseline dynamic PET experiments (Brust et al. 2008). In the thalamus the BP's of (+)-[ $^{18}\text{F}$ ]NCFHEB, (-)-[ $^{18}\text{F}$ ]NCFHEB and 2-[ $^{18}\text{F}$ ]FA were 7.6, 2.5 and 1.6, correspondingly. The brain uptake was higher for (+)-[ $^{18}\text{F}$ ]NCFHEB ( $\text{SUV} = 8$ ) and (-)-[ $^{18}\text{F}$ ]NCFHEB ( $\text{SUV} \sim 5$ ) and

Table 2

In vitro and PET imaging properties of [ $^{18}\text{F}$ ]JHU85208, [ $^{18}\text{F}$ ]JHU85157 and [ $^{18}\text{F}$ ]JHU85270 (Gao et al. 2007c).

Ligand	$K_i$ , nM <sup>a</sup> ( $K_{\text{rel}}^b$ )	$\log D_{7.4}^c$	Peak uptake in thalamus <sup>d</sup>	BP
[ $^{11}\text{C}$ ]JHU85208	0.05; 0.06 (0.9)	$1.83 \pm 0.02$	10 min	0.7 <sup>th</sup>
[ $^{11}\text{C}$ ]JHU85157	0.02; 0.05 (0.6)	$2.28 \pm 0.05$	10 min	0.8 <sup>th</sup>
[ $^{11}\text{C}$ ]JHU85270	0.090 (1.9)	$1.60 \pm 0.08$	30 min	0.7 <sup>th</sup>

<sup>a</sup>The inhibition binding affinity was determined commercially by NovaScreen (Hanover, MD) using rat cortical membranes and [ $^3\text{H}$ ]epibatidine; <sup>b</sup> $K_{\text{rel}}$ , a ratio of the  $K_i$  for the test compound to that of (-)-epibatidine from the same assay run. The  $K_i$  values of (-)-epibatidine, a standard ligand, varied from 0.04 to 0.07 nM in the parallel assays; <sup>c</sup>The partition coefficients between octanol and sodium phosphate buffer at pH 7.4 ( $\log D_{7.4}$ ) were determined experimentally in quadruplicate. Data are mean  $\pm$  S.D. ( $n = 4$ ). Abbreviation: Th = thalamus; <sup>d</sup>All PET studies have been performed in the adult male baboons.

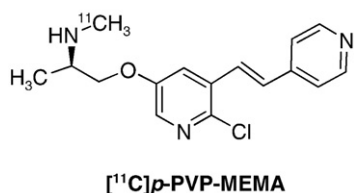


Fig. 5. Structure of (R,E)-1-(6-chloro-5-(2-(pyridin-4-yl)vinyl)pyridin-3-yloxy)-N-[ $^{11}\text{C}$ ]methylpropan-2-amine ([ $^{11}\text{C}$ ]p-PVP-MEMA).

lower for 2-[ $^{18}\text{F}$ ]FA (SUV ~2.5). The accumulation of radioactivity of (+)-[ $^{18}\text{F}$ ]NCFHEB, (-)-[ $^{18}\text{F}$ ]NCFHEB and 2-[ $^{18}\text{F}$ ]FA in pig thalamus peaked at 142 min, 80 min and 68 min, correspondingly. Despite the seemingly slower kinetics of (-)-[ $^{18}\text{F}$ ]NCFHEB vs. 2-[ $^{18}\text{F}$ ]FA in the pig thalamus the authors of the paper (Brust et al. 2008) concluded that the binding equilibrium of (-)-[ $^{18}\text{F}$ ]NCFHEB was reached faster than that of 2-[ $^{18}\text{F}$ ]FA. The conclusion was based on the thalamus/olfactory bulb ratio vs. time dependence (peak at 2 h for (-)-[ $^{18}\text{F}$ ]NCFHEB and 3.3 h for 2-[ $^{18}\text{F}$ ]FA). The authors concluded that the faster brain kinetics of (-)-[ $^{18}\text{F}$ ]NCFHEB may be advantageous in comparison with 2-[ $^{18}\text{F}$ ]FA. No further studies with (-)-[ $^{18}\text{F}$ ]NCFHEB have been published yet. It is possible that (-)-[ $^{18}\text{F}$ ]NCFHEB may have a potential for clinical application if quantitative PET experiments in non-human primates provide evidence of more rapid brain kinetics of (-)-[ $^{18}\text{F}$ ]NCFHEB vs. 2-[ $^{18}\text{F}$ ]FA.

#### [ $^{18}\text{F}$ ]AZAN ([ $^{18}\text{F}$ ]JHU87522) and its analogs

Continuing efforts to develop a radioligand with “rapid” brain kinetics and improved BP led the Johns Hopkins group to a series of nAChR antagonists (Fig. 6), analogs of epibatidine (Gao et al. 2007a, 2008b). At least one compound of the series, (-)-2-(6-[ $^{18}\text{F}$ ]fluoro-2,3'-bipyridin-5'-yl)-7-methyl-7-aza-bicyclo[2.2.1]heptane ([ $^{18}\text{F}$ ]JHU87522 or [ $^{18}\text{F}$ ]AZAN) exhibited better imaging properties in animal studies than those of 2-[ $^{18}\text{F}$ ]FA and 6-[ $^{18}\text{F}$ ]FA including a greater BP value and faster brain kinetics. In addition, the brain uptake of [ $^{18}\text{F}$ ]AZAN is greater and its acute toxicity is lower. Details on the imaging properties and the rationale for development of [ $^{18}\text{F}$ ]AZAN and its analogs are provided below.

Balancing the in vitro and in vivo properties was important for the success of this project (Table 3). The radioligand, [ $^{11}\text{C}$ ]-JHU86328 (Fig. 6), with highest binding affinity and lipophilicity values within the series exhibited high tissue/cerebellum ratio in the rat brain (Table 3) (Gao et al. 2007a). MicroPET studies with [ $^{11}\text{C}$ ]-JHU86328 produced encouraging images that were suitable for nAChR mapping of the thalamus and cortex of the rat brain. However, in the baboon PET study the radioligand [ $^{11}\text{C}$ ]-JHU86328 demonstrated only a moderate thalamus/cerebellum ratio. The accumulation of [ $^{11}\text{C}$ ]-JHU86328 radioactivity failed to reach steady-state in the baboon thalamus within 90 min post-injection. The authors of the paper concluded that structural analogs of [ $^{11}\text{C}$ ]-JHU86328 with reduced binding affinity

**Table 3**

In vitro and PET imaging properties of [ $^{18}\text{F}$ ]AZAN analogues (Gao et al. 2007a, 2008b).

Ligand	$K_i$ , nM ( $K_{rel}^b$ )	$\log D_{7.4}^c$	Peak uptake in thalamus <sup>f</sup>	BP	Scanning time for accurate quantification of nAChR, h
2-[ $^{18}\text{F}$ ]FA	1.33 (22)	-1.4	>270 min <sup>a</sup>	2 <sup>Th</sup>	5–6 <sup>Th</sup>
[ $^{11}\text{C}$ ]-(-)-JHU86328	0.016, 0.017 (0.4)	1.26	>90 min	>1 <sup>Th</sup>	d
[ $^{11}\text{C}$ ]-(-)-JHU86358	0.05;	0.46 ± 0.07	>90 min	>2 <sup>Th</sup>	d
[ $^{18}\text{F}$ ]-(-)-JHU86358	0.05 (1.0)		>180 min	>7 <sup>Th</sup> 1.1 <sup>Cx</sup>	~3 <sup>Th</sup> , 1.5 <sup>Ctx</sup>
[ $^{18}\text{F}$ ]-(-)-JHU86430	0.061; 0.052 (1.3)	0.67 ± 0.02	160 min	>7 <sup>Th</sup> 1.0 <sup>Cx</sup>	~3 <sup>Th</sup> , 1.5 <sup>Ctx</sup>
[ $^{18}\text{F}$ ]-(-)-JHU86428 ([ $^{18}\text{F}$ ]XTRA)	0.113; 0.133 (2.0)	0.74 ± 0.02	65–70 min	7.3 <sup>Th</sup> 1.3 <sup>Cx</sup>	2–2.5 <sup>Th</sup> , 1 <sup>Ctx</sup>
[ $^{18}\text{F}$ ]-(-)-JHU87522 ([ $^{18}\text{F}$ ]AZAN)	0.310; 0.339 (4.4)	0.99 ± 0.05	7–28 min	2.1–4.8 <sup>Th</sup> 0.6–1.0 <sup>Cx</sup>	1.5 <sup>Th</sup> , 1.5 <sup>Ctx</sup>

<sup>a</sup>In vivo data with 2-[ $^{18}\text{F}$ ]FA have obtained in Rhesus monkey PET studies (Chefer et al. 2003); <sup>b</sup> $K_{rel}$ , a ratio of the  $K_i$  for the test compound to that of (-)-epibatidine from the same assay run. The  $K_i$  values of (-)-epibatidine, a standard ligand, varied from 0.04 to 0.07 nM in the parallel assays; <sup>c</sup>The partition coefficients between octanol and sodium phosphate buffer at pH 7.4 ( $\log D_{7.4}$ ); <sup>d</sup>The required scanning time (>1.5–2 h) is greater than it is practical for  $^{11}\text{C}$ ; <sup>e</sup>All PET studies have been performed in the adult male baboons, 15–27 kg. The bolus doses of  $^{11}\text{C}$ - and  $^{18}\text{F}$ -radioligands were 10–12 mCi and 6–10 mCi (specific radioactivity range was 4300–11,000 mCi/μmol); Abbreviation: Th = thalamus, Ctx = cortex.

(to accelerate the radioligand brain kinetics) and reduced lipophilicity (to diminish the non-specific binding) should be synthesized.

The des-chloro analogs of (-)-JHU86328, isomers (-)-JHU86358, (-)-JHU86428, (-)-JHU86430 and (-)-JHU87522 (Fig. 6), exhibited lower lipophilicity and a wide range of binding affinities (Table 3). (-)-JHU86358, the isomer with highest binding affinity, was radiolabeled with  $^{11}\text{C}$  and  $^{18}\text{F}$ . Although [ $^{11}\text{C}$ ]-JHU86358 did not reach steady-state in the baboon thalamus within the 1.5 h of the PET study, its imaging properties including thalamus/cerebellum ratio were better than those of [ $^{11}\text{C}$ ]-JHU86328. The results of the baboon PET experiments (Gao et al. 2007a) with [ $^{18}\text{F}$ ]-JHU86358, an isotopomer of [ $^{11}\text{C}$ ]-JHU86358 with longer half-life, suggested that the  $^{18}\text{F}$ -radioligand displayed very high binding potentials for a nAChR radioligand (Table 3) and more rapid brain kinetics than [ $^{18}\text{F}$ ]NIDA522131 ((S)-5-(azetidin-2-ylmethoxy)-2-chloro-2'-[ $^{18}\text{F}$ ]fluoro-3,4'-bipyridine) (Fig. 2), the azetidine-based nAChR radioligand (Zhang and Horti 2004) with equally high BP values but very slow brain kinetics (Chefer et al. 2008). However, further PET modeling did not convince the investigators that the brain kinetics of [ $^{18}\text{F}$ ]-JHU86358 were sufficiently rapid for practical applications. In addition, [ $^{18}\text{F}$ ]-JHU86430, an isomer of [ $^{18}\text{F}$ ]-JHU86358 with almost equivalent binding affinity, exhibited similar imaging properties in a single baboon study when compared with [ $^{18}\text{F}$ ]-JHU86358 (Gao et al. 2008b). It appeared that a radioligand with even lower binding affinity might be necessary and the remaining two isomers of the series, [ $^{18}\text{F}$ ]-JHU86428 and [ $^{18}\text{F}$ ]-JHU87522 (Fig. 6), looked promising.

[ $^{18}\text{F}$ ]-JHU86428 ((-)-2-(2'-[ $^{18}\text{F}$ ]fluoro-3,3'-bipyridin-5'-yl)-7-methyl-7-aza-bicyclo[2.2.1]heptane, [ $^{18}\text{F}$ ]XTRA), an isomer exhibiting 50% of the binding affinity of [ $^{18}\text{F}$ ]-JHU86358 (Table 3), readily entered baboon brain and peaked at 75 min post injection. The BP value in thalamus and cortex were high (Table 3) and PET modeling demonstrated that the radioligand reached steady-state in the thalamus and cortex at about 2.5 h and 1.5 h post-injection, respectively (Gao et al. 2008b). [ $^{18}\text{F}$ ]XTRA is considered as a promising candidate for imaging of extrathalamic nAChR in humans and more studies are warranted to support this claim.

The isomer [ $^{18}\text{F}$ ]-JHU87522 (Gao et al. 2008b) ((-)-2-(6-[ $^{18}\text{F}$ ]fluoro-2,3'-bipyridin-5'-yl)-7-methyl-7-aza-bicyclo[2.2.1]heptane, [ $^{18}\text{F}$ ]AZAN) had the lowest binding affinity within the series (but still quite high) (Table 3). In two baseline and one blockade PET experiments in baboon [ $^{18}\text{F}$ ]AZAN exhibited properties of highly specific

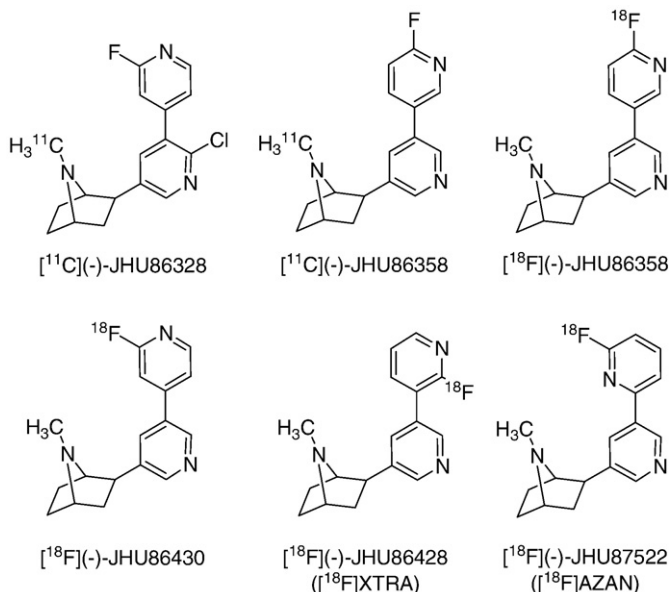


**Fig. 6.** The dipyrindyl-azabicyclo[2.2.1]heptane series of the Johns Hopkins group.

nAChR radioligand with the optimally rapid brain kinetics, high BP and high uptake (%SUV) (Fig. 7, Table 3). Most nAChR radioligands with similarly rapid kinetics exhibited low values of BP and, *vice versa*, radioligands with high BP values were slow in the brain regions with high density of nAChR (Brown et al. 2001, 2002, 2004; Ding et al. 2006; Horti and Villemagne 2006; Kozikowski et al. 2006; Pichika et al. 2006; Roger et al. 2006). PET modeling (Fig. 7, right) demonstrated that only ~90 min of scanning was required for a robust estimation of outcome variables of [ $^{18}\text{F}$ ]AZAN with 95% accuracy including volume of distribution and BP in thalamus, the region with highest density of nAChR. For comparison, at least 6 h was needed for 2-[ $^{18}\text{F}$ ]FA (Fig. 7, right), the only available nAChR radioligand for humans. In addition, [ $^{18}\text{F}$ ]AZAN exhibited greater total brain uptake (Fig. 7, left) than that of 2-[ $^{18}\text{F}$ ]FA (Fig. 1) suggesting that a lower dose of [ $^{18}\text{F}$ ]AZAN will be required for a PET study and [ $^{18}\text{F}$ ]AZAN may likely represent a lower radiation burden to animals and human research subjects.

It is the present hypothesis that within the series of four isomeric radioligands [ $^{18}\text{F}$ ](–)-JHU86358, [ $^{18}\text{F}$ ](–)-JHU86428 ([ $^{18}\text{F}$ ]XTRA), [ $^{18}\text{F}$ ](–)-JHU86430 and [ $^{18}\text{F}$ ](–)-JHU87522 ([ $^{18}\text{F}$ ]AZAN) shown in Fig. 6 the isomer [ $^{18}\text{F}$ ]AZAN exhibited most “rapid” brain kinetics because of its relatively low binding affinity and high lipophilicity. There may be some other differences in the properties of the isomers including the rate of association/dissociation that may contribute to their brain kinetics dissimilarities.

### Further preclinical studies with [ $^{18}\text{F}$ ](–)-JHU87522 ([ $^{18}\text{F}$ ]AZAN)

#### Metabolism studies in mice and baboon

HPLC blood analysis demonstrated that [ $^{18}\text{F}$ ](–)-JHU87522 ([ $^{18}\text{F}$ ]AZAN) undergoes metabolism in mice and baboon producing three hydrophilic radiometabolites. HPLC analysis of the mouse brain extract showed that about 7% of one of the radiometabolites penetrates the blood–brain barrier. Because the relative amount of this metabolite in baboon blood was 6-fold lower than that in mice, the authors of the paper (Gao et al. 2008b) concluded that the concentration of the metabolite in baboon brain was not significant and could be ignored in the PET modeling.

#### nAChR-subtype inhibition binding assay

It is well known that toxicological properties of nAChR ligands are associated with activation of the ganglionic  $\alpha 3\beta 4$ -nAChR (Holladay et al. 1997). Inhibition binding assay of (–)-JHU87522 (AZAN) and 2-

**Table 4**

Comparison of  $K_i$  values (Gao et al. 2008b) of binding of (±)-epibatidine, a high affinity reference ligand, 2-FA, the only available ligand for PET imaging of nAChR in humans, and the novel compound (–)-JHU87522 (AZAN) to membrane homogenates from six stably transfected cell lines expressing six subtypes of nAChRs.

Ligand	$K_i$ , nM						$\alpha 3\beta 4/\alpha 4\beta 2$
	$\alpha 4\beta 2$	$\alpha 2\beta 2$	$\alpha 2\beta 4$	$\alpha 3\beta 2$	$\alpha 3\beta 4$	$\alpha 4\beta 4$	
Epibatidine	0.061	0.025	0.095	0.035	0.57	0.16	13
2-FA	1.33	1.44	181	3.02	3680	188	2767
[ $^{18}\text{F}$ ](–)-JHU87522 ([ $^{18}\text{F}$ ]AZAN)	0.26	0.26	7.8	4	310	6.2	0.95

The data suggest that (–)-JHU87522 (AZAN) is a  $\beta 2$ -nAChR-selective ligand with higher  $\alpha 4\beta 2$ -nAChR binding affinity than that of 2-FA. Low binding of (–)-JHU87522 (AZAN) to ganglionic  $\alpha 3$ -nAChR subtypes explains in part the low toxic effect of (–)-JHU87522 (AZAN) in mice.

FA with various nAChR subtypes has been performed (Gao et al. 2008b) (Table 4). The study showed that (–)-JHU87522 (AZAN) displayed a binding affinity between the high affinity epibatidine and the less potent 2-FA. Unlike the very toxic epibatidine, both compounds (–)-JHU87522 (AZAN) and 2-FA are  $\alpha 4\beta 2$ -nAChR selective versus  $\alpha 3\beta 4$ -nAChR subtype (Table 4). This finding is in agreement with the low toxicity of the latter ligands (see also the Safety studies below).

#### *In vitro* functional assay of [ $^{18}\text{F}$ ](–)-JHU87522 ([ $^{18}\text{F}$ ]AZAN)

$\alpha 4\beta 2$ -nAChR functional assays were performed using the SH-EP1 cell line stably transfected with the human  $\alpha 4\beta 2$ -nAChR (Gao et al. 2008b). The results of the assay demonstrated that (–)-JHU87522 (AZAN) antagonized the effect of 30  $\mu\text{M}$  acetylcholine (ACh) at  $\alpha 4\beta 2$ -nAChR with  $K_D$  value of 0.54 nM and, thus, (–)-JHU87522 (AZAN) exhibited functional properties of potent antagonist of  $\alpha 4\beta 2$ -nAChR subtype.

#### Preliminary safety studies with [ $^{18}\text{F}$ ](–)-JHU87522 ([ $^{18}\text{F}$ ]AZAN)

Most available PET and SPECT imaging agents for nAChR are agonists. These nAChR-agonists are toxic when injected at high doses. Nicotinic agonists that show little nAChR-subtype selectivity (for example 6-fluoropyridin-3-yl-7-azabicyclo[2.2.1]heptane (FPH)) and display high binding affinity with both, cerebral  $\alpha 4\beta 2$ -nAChR and ganglionic  $\alpha 3\beta 4$ -nAChR, are very toxic. Highly selective  $\alpha 4\beta 2$ -nAChR agonists such as 2-FA and 5-IA manifest substantially lower toxicity and can be used in human imaging studies if injected at tracer doses. (Fisher et al. 1994; Molina et al. 1997; Horti et al. 1998b,c; Vaupel et al.

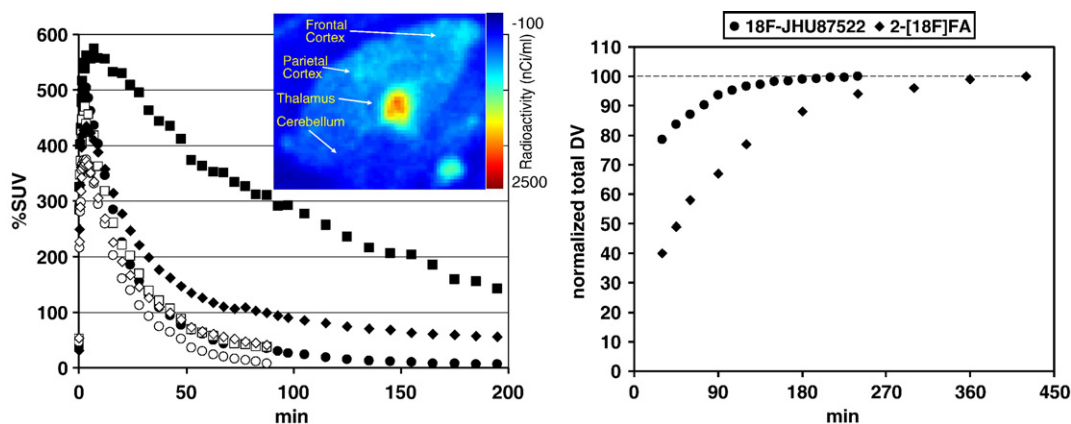
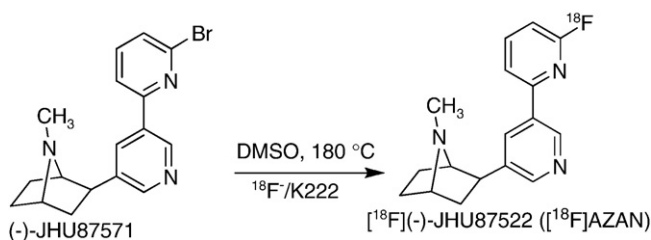


**Fig. 7.** Left: Regional brain time-uptake curves of [ $^{18}\text{F}$ ](–)-JHU87522 ([ $^{18}\text{F}$ ]AZAN) in baboon (22 kg male). Squares = thalamus, circles = cerebellum, diamonds = cortex. Filled symbols = baseline study (6 mCi, specific activity (s.a.) = 5300 mCi/ $\mu\text{mol}$ ); open symbols = blockade study (7 mCi, s.a. = 4800 mCi/ $\mu\text{mol}$ ) with cytosine (2 mg/kg, s.c.). Both studies were performed in the same animal. Insert: Averaged (10–90 min) baseline PET image in sagittal view; Right: Comparison of total distribution volumes in thalamus ( $DV_T$ ) of 2-[ $^{18}\text{F}$ ]FA (the data are adopted from (Chefer et al. 2003)) and [ $^{18}\text{F}$ ](–)-JHU87522 ([ $^{18}\text{F}$ ]AZAN) (Gao et al. 2008b) as functions of scanning time. At 90-min, estimates of  $DV_T$  reached 95% and 67% of the maximum value for [ $^{18}\text{F}$ ](–)-JHU87522 ([ $^{18}\text{F}$ ]AZAN) and 2-[ $^{18}\text{F}$ ]FA, respectively.





**Scheme 1.** Radiosynthesis of [ $^{18}\text{F}$ ]( $-$ )-JHU87522 ([ $^{18}\text{F}$ ]AZAN) is simple (one-step) and it can be performed in an nucleophilic fluorination radiochemistry box.

2003, 2005) ( $-$ )-JHU87522 (AZAN) is a highly selective  $\alpha 4\beta 2$ - versus  $\alpha 3\beta 4$ -subtype nAChR ligand. In addition, unlike the currently available for clinic nAChR PET radioligands (Table 1) AZAN is a nAChR antagonist (see above). Taking into consideration the subtype selectivity and functional activity of AZAN one can infer its low toxicity. In the blocking experiment intravenous injection of AZAN in mice at doses of 2, 50 and 200 nmol/kg did not produce noticeable adverse effects. At an i.v. dose of 2  $\mu\text{mol/kg}$  mice displayed reduced locomotor activity and Straub tail with full recovery in 10 min post injection. This preliminary assessment of toxicological properties of AZAN demonstrated that this compound exhibits at least the same or lower acute toxicity than that of 2-FA and merits further development (Gao et al. 2008b). Currently AZAN is undergoing toxicological studies that will determine if this radioligand is sufficiently safe for clinical application as a PET radiotracer.

#### Synthesis of [ $^{18}\text{F}$ ]( $-$ )-JHU87522 ([ $^{18}\text{F}$ ]AZAN)

Radiolabeling of [ $^{18}\text{F}$ ]( $-$ )-JHU87522 ([ $^{18}\text{F}$ ]AZAN) was performed remotely in one step by radiofluorination of corresponding bromo derivative ( $-$ )-JHU87571 (Scheme 1) using an FDG radiochemistry box (MicroLab, GE) (Gao et al. 2008b). The final product [ $^{18}\text{F}$ ]( $-$ )-JHU87522 ([ $^{18}\text{F}$ ]AZAN) was prepared with high radiochemical yield  $39 \pm 8\%$  and specific radioactivity  $7400 \pm 1300$  mCi/ $\mu\text{mol}$  (EOS). Lacking a final product deprotection step required in other radiotracer syntheses, the radiosynthesis of [ $^{18}\text{F}$ ]( $-$ )-JHU87522 ([ $^{18}\text{F}$ ]AZAN) is substantially simpler than the syntheses of 2-[ $^{18}\text{F}$ ]FA or 6-[ $^{18}\text{F}$ ]FA (Dolle et al. 1998; Horti et al. 1998a, 2000; Ding et al. 2000; Schmaljohann et al. 2004). The relative ease of the radiochemistry is another important advantage of [ $^{18}\text{F}$ ]AZAN.

#### Conclusion

Development of the nAChR PET radioligands with optimal brain kinetics will facilitate further nicotinic imaging studies in smoking, epilepsy, ADHD, depression, schizophrenia, cognition, behavior, memory, and, especially, in research of aging, cognitive impairments, and dementia because of the hindrance of performing lengthy studies with the currently available radioligands in elderly and cognitively impaired. These new imaging probes should also assist and accelerate the progress in the development of nAChR-acting drugs that are under development by the pharmaceutical industry. Currently 2-[ $^{18}\text{F}$ ]FA is the only available clinical radiotracer for the PET quantification of cerebral nAChR, the major receptor in mammalian brain. However, slow brain kinetics and low binding potentials are the substantial drawbacks of 2-[ $^{18}\text{F}$ ]FA that preclude widespread use of PET imaging research of nAChR in humans.

The majority of the recent publications on the development of nAChR radioligands has focused on the development of the radioligands with improved kinetics properties in comparison with 2-[ $^{18}\text{F}$ ]FA. Several PET groups around the world have presented a variety of radioligands with fast regional brain kinetics in non-human primates and pigs. The most promising compounds are ( $-$ )-[ $^{18}\text{F}$ ]NCFHEB and [ $^{18}\text{F}$ ]AZAN.

PET studies in pig showed that in comparison with 2-[ $^{18}\text{F}$ ]FA ( $-$ )-[ $^{18}\text{F}$ ]NCFHEB displayed a 100% greater brain uptake, 50% higher  $\text{BP}^{\text{Thalamus}}$  values and may reach steady-state sooner. Yet, in order to consider ( $-$ )-[ $^{18}\text{F}$ ]NCFHEB for further pre-clinical development additional PET studies have to confirm the imaging advantage of ( $-$ )-[ $^{18}\text{F}$ ]NCFHEB versus the currently available radioligands. These experiments should include quantitative PET imaging in non-human primates to provide evidence of more rapid brain kinetics in comparison with 2-[ $^{18}\text{F}$ ]FA.

The available pre-clinical data on [ $^{18}\text{F}$ ]( $-$ )-JHU87522 ([ $^{18}\text{F}$ ]AZAN) suggest that this radioligand is superior to 2-[ $^{18}\text{F}$ ]FA for quantitative PET imaging of  $\alpha 4\beta 2$ -nAChR. In baboon PET studies [ $^{18}\text{F}$ ]AZAN exhibits 200–300% greater brain uptake, 35–100% higher BPs and reaches steady-state in approximately 1.5 h post-bolus administration versus 6–8 h for 2-[ $^{18}\text{F}$ ]FA. In vitro binding assay shows greater binding affinity of AZAN and similar nAChR-subtype selectivity in comparison with 2-FA. Both ligands bind selectively with  $\beta 2$ -subtypes that are predominant nAChR subtypes in the mammal brain and display little binding affinity at ganglionic  $\alpha 3\beta 4$ -nAChR. Unlike 2-FA that is nAChR agonist, AZAN displays properties of functional antagonist of  $\alpha 4\beta 2$ -nAChR. The preliminary safety experiments demonstrate that AZAN manifest similar or lower acute toxicity versus 2-FA. The relative ease of the radiochemistry (one-step) is another important advantage of [ $^{18}\text{F}$ ]AZAN in comparison with 2-[ $^{18}\text{F}$ ]FA (two-step). Overall [ $^{18}\text{F}$ ]AZAN holds promise as better PET radioligand than 2-[ $^{18}\text{F}$ ]FA. The combination of these properties of [ $^{18}\text{F}$ ]AZAN justify further pre-clinical development. At this time [ $^{18}\text{F}$ ]AZAN is undergoing pre-IND toxicology and radiation dosimetry experiments. If [ $^{18}\text{F}$ ]AZAN is safe for human PET studies, there are strong indications that it could become the radiotracer of choice for PET imaging of nAChR in human brain.

#### Acknowledgements

The authors are grateful to Drs. Rao Rapaka and Thomas Aigner (NIDA, NIH) for fruitful discussions. Preparation of this article was supported in part by the NIH Grant DA020777 (AGH) and Division of Nuclear Medicine of the Johns Hopkins School of Medicine.

#### References

- Alavi A, Basu S. Planar and SPECT imaging in the era of PET and PET-CT: Can it survive the test of time? *European Journal of Nuclear Medicine and Molecular Imaging* 35 (8), 1554–1559, 2008.
- Bottlaender M, Valette H, Roumenov D, Dolle F, Coulon C, Ottaviani M, Hinnen F, Ricard M. Biodistribution and radiation dosimetry of 18F-fluoro-A-85380 in healthy volunteers. *Journal of Nuclear Medicine* 44 (4), 596–601, 2003.
- Brody AL, Mandelkern MA, London ED, Olmstead RE, Farahi J, Scheibel D, Jou J, Allen V, Tongson E, Chefer SI, Koren AO, Mukhin AG. Cigarette smoking saturates brain  $\alpha 4\beta 2$  nicotinic acetylcholine receptors. *Archives of General Psychiatry* 63 (8), 907–915, 2006.
- Brown LL, Pavlova O, Mukhin A, Kimes AS, Horti AG. Radiosynthesis of 5-[2-(4-pyridinyl)vinyl]-6-chloro-3-[(1-[ $^{11}\text{C}$ ]methyl-2-(S)-pyrrolidinyl)methoxy]pyridine, a high affinity ligand for studying nicotinic acetylcholine receptors by positron emission tomography. *Bioorganic and Medicinal Chemistry* 9 (11), 3055–3058, 2001.
- Brown LL, Kulkarni S, Pavlova OA, Koren AO, Mukhin AG, Newman AH, Horti AG. Synthesis and evaluation of a novel series of 2-chloro-5-[(1-methyl-2-(S)-pyrrolidinyl)methoxy]-3-(2-(4-pyridinyl)vinyl) pyridine analogues as potential positron emission tomography imaging agents for nicotinic acetylcholine receptors. *Journal of Medicinal Chemistry* 45 (13), 2841–2849, 2002.
- Brown L, Chefer S, Pavlova O, Vaupel DB, Koren AO, Kimes AS, Horti AG, Mukhin AG. Evaluation of 5-(2-(4-pyridinyl)vinyl)-6-chloro-3-(1-methyl-2-(S)-pyrrolidinyl-methoxy)pyridine and its analogues as PET radioligands for imaging nicotinic acetylcholine receptors. *Journal of Neurochemistry* 91 (3), 600–612, 2004.
- Brust P, Patt JT, Deuther-Conrad W, Becker G, Patt M, Schildan A, Sorger D, Kendziorra K, Meyer P, Steinbach J, Sabri O. In vivo measurement of nicotinic acetylcholine receptors with [ $^{18}\text{F}$ ]norchloro-fluoro-homoepibatidine. *Synapse* 62 (3), 205–218, 2008.
- Carroll FI, Ware R, Brieady LE, Navarro HA, Damaj MI, Martin BR. Synthesis, nicotinic acetylcholine receptor binding, and antinociceptive properties of 2'-fluoro-3'-(substituted phenyl)deschloroepibatidine analogues. Novel nicotinic antagonist. *Journal of Medicinal Chemistry* 47 (18), 4588–4594, 2004.
- Carroll FI, Ma W, Yokota Y, Lee JR, Brieady LE, Navarro HA, Damaj MI, Martin BR. Synthesis, nicotinic acetylcholine receptor binding, and antinociceptive properties of 3'-substituted deschloroepibatidine analogues. Novel nicotinic antagonists. *Journal of Medicinal Chemistry* 48 (4), 1221–1228, 2005.



- Carson RE, Channing MA, Blasberg RG, Dunn BB, Cohen RM, Rice KC, Herscovitch P. Comparison of bolus and infusion methods for receptor quantitation: Application to [ $^{18}\text{F}$ ]cyclohexyl and positron emission tomography. *Journal of Cerebral Blood Flow and Metabolism* 13 (1), 24–42, 1993.
- Chefer SI, London ED, Koren AO, Pavlova OA, Kurian V, Kimes AS, Horti AG, Mukhin AG. Graphical analysis of 2-[ $^{18}\text{F}$ ]FA binding to nicotinic acetylcholine receptors in rhesus monkey brain. *Synapse* 48 (1), 25–34, 2003.
- Chefer SI, Pavlova OA, Zhang Y, Vaupel DB, Kimes AS, Horti AG, Stein E, Mukhin AG. NIDA522131, a new radioligand for imaging extrathalamic nicotinic acetylcholine receptors: In vitro and in vivo evaluation. *Journal of Neurochemistry* 104, 306–315, 2008.
- Deuther-Conrad W, Patt JT, Feuerbach D, Wegner F, Brust P, Steinbach J. Norchloro-fluoro-homoepibatidine: specificity to neuronal nicotinic acetylcholine receptor subtypes in vitro. *Farmaco* 59 (10), 785–792, 2004.
- Deuther-Conrad W, Patt JT, Lockman PR, Allen DD, Patt M, Schildan A, Ganapathy V, Steinbach J, Sabri O, Brust P. Norchloro-fluoro-homoepibatidine (NCFHEB) – a promising radioligand for neuroimaging nicotinic acetylcholine receptors with PET. *European Neuropsychopharmacology* 18 (3), 222–229, 2008.
- Ding YS, Fowler J. New-generation radiotracers for nAChR and NET. *Nuclear Medicine and Biology* 32 (7), 707–718, 2005.
- Ding YS, Liu N, Wang T, Marecek J, Garza V, Ojima I, Fowler JS. Synthesis and evaluation of 6-[ $^{18}\text{F}$ ]fluoro-3-(2(S)-azetidinylmethoxy)pyridine as a PET tracer for nicotinic acetylcholine receptors. *Nuclear Medicine and Biology* 27 (4), 381–389, 2000.
- Ding YS, Fowler JS, Logan J, Wang GJ, Telang F, Garza V, Bieganski A, Pareto D, Rooney W, Shea C, Alexoff D, Volkow ND, Vocci F. 6-[ $^{18}\text{F}$ ]Fluoro-A-85380, a new PET tracer for the nicotinic acetylcholine receptor: Studies in the human brain and in vivo demonstration of specific binding in white matter. *Synapse* 53 (3), 184–189, 2004.
- Ding YS, Kil KE, Lin KS, Ma W, Yokota Y, Carroll IF. A novel nicotinic acetylcholine receptor antagonist radioligand for PET studies. *Bioorganic and Medicinal Chemistry Letters* 16 (4), 1049–1053, 2006.
- Dolle F, Valette H, Bottlaender M, Hinnen F, Vaufrey F, Guenther I, Crouzel C. Synthesis of 2-[ $^{18}\text{F}$ ]fluoro-3-[2(S)-2-azetidinylmethoxy]pyridine, a highly potent radioligand for in vivo imaging central nicotinic acetylcholine receptors. *Journal of Labelled Compounds & Radiopharmaceuticals* 41 (5), 451–456, 1998.
- Dolle F, Langle S, Roger G, Fulton RR, Lagnel-de Bruin B, Henderson DJ, Hinnen F, Paine T, Coster MJ, Valette H, Bottlaender M, Kassiou M. Synthesis and in-vivo evaluation of [11C]p-PVP-MEMA as a PET radioligand for imaging nicotinic receptors. *Australian Journal of Chemistry* 61 (6), 438–445, 2008.
- Easwaramoorthy B, Pichika R, Collins D, Potkin SG, Leslie FM, Mukherjee J. Effect of acetylcholinesterase inhibitors on the binding of nicotinic alpha4beta2 receptor PET radiotracer, (18F)-nifene: A measure of acetylcholine competition. *Synapse* 61 (1), 29–36, 2007.
- Ellis JR, Villemagne VL, Nathan PJ, Mulligan RS, Gong SJ, Chan JG, Sachinidis J, O'Keefe GJ, Pathmaraj K, Wesnes KA, Savage G, Rowe CC. Relationship between nicotinic receptors and cognitive function in early Alzheimer's disease: A 2-[ $^{18}\text{F}$ ]fluoro-A-85380 PET study. *Neurobiology of Learning and Memory* 90 (2), 404–412, 2008.
- Fisher M, Huangfu D, Shen TY, Guyenet PG. Epibatidine, an alkaloid from the poison frog *Epipedobates tricolor*, is a powerful ganglionic depolarizing agent. *Journal of Pharmacology and Experimental Therapeutics* 270 (2), 702–707, 1994.
- Gao Y, Horti AG, Kuwabara H, Ravert HT, Hilton J, Holt DP, Kumar A, Alexander M, Endres CJ, Wong DF, Dannals RF. Derivatives of (-)-7-methyl-2-(5-(pyridinyl)pyridin-3-yl)-7-azabicyclo[2.2.1]heptane are potential ligands for positron emission tomography imaging of extrathalamic nicotinic acetylcholine receptors. *Journal of Medicinal Chemistry* 50 (16), 3814–3824, 2007a.
- Gao Y, Ravert HT, Holt D, Dannals RF, Horti AG. 6-Chloro-3-(((1-[11C]methyl)-2-(S)-pyrrolidinyl)methoxy)-5-(2-fluoropyridin-4-yl)pyridine ([11C]HU58270), a potent ligand for nicotinic acetylcholine receptor imaging by positron emission tomography. *Applied Radiation and Isotopes* 65 (8), 947–951, 2007b.
- Gao Y, Ravert HT, Holt DP, Hilton J, Endres C, Alexander M, Kumar A, Pomper MG, Rahmim A, Kuwabara H, Wong DF, Dannals RF, Horti AG. Synthesis and initial evaluation of novel dipyrilidyl derivatives as potential radioligands for imaging of the nicotinic acetylcholine receptors by positron-emission tomography (PET). Abstracts of Papers, 233 rd ACS National Meeting, Chicago, IL, United States, March 25–29, 2007c, MEDI-289.
- Gao Y, Horti AG, Kuwabara H, Ravert HT, Holt DP, Kumar A, Alexander M, Wong DF, Dannals RF. New synthesis and evaluation of enantiomers of 7-methyl-2-exo-(3'-iodo-5'-pyridinyl)-7-azabicyclo[2.2.1]heptane as stereoselective ligands for PET imaging of nicotinic acetylcholine receptors. *Bioorganic and Medicinal Chemistry Letters* 18 (23), 6168–6170, 2008a.
- Gao Y, Kuwabara H, Spivak CE, Xiao Y, Kellar K, Ravert HT, Kumar A, Alexander M, Hilton J, Wong DF, Dannals RF, Horti AG. Discovery of (-)-7-methyl-2-exo-[3'-(6-[ $^{18}\text{F}$ ]fluoropyridin-2-yl)-5'-pyridinyl]-7-azabicyclo[2.2.1]heptane, a radiolabeled antagonist for cerebral nicotinic acetylcholine receptor (alpha4beta2-nAChR) with optimal positron emission tomography imaging properties. *Journal of Medicinal Chemistry* 51 (15), 4751–4764, 2008b.
- Gotti C, Fornasari D, Clementi F. Human neuronal nicotinic receptors. *Progress in Neurobiology* 53 (2), 199–237, 1997.
- Gotti C, Riganti L, Vailati S, Clementi F. Brain neuronal nicotinic receptors as new targets for drug discovery. *Current Pharmaceutical Design* 12 (4), 407–428, 2006.
- Gundisch D. Nicotinic acetylcholine receptors and imaging. *Current Pharmaceutical Design* 6 (11), 1143–1157, 2000.
- Gundisch D, Koren AO, Horti AG, Pavlova OA, Kimes AS, Mukhin AG, London ED. In vitro characterization of 6-[ $^{18}\text{F}$ ]fluoro-A-85380, a high-affinity ligand for alpha4beta2\* nicotinic acetylcholine receptors. *Synapse* 55 (2), 89–97, 2005.
- Holladay MW, Dart MJ, Lynch JK. Neuronal nicotinic acetylcholine receptors as targets for drug discovery. *Journal of Medicinal Chemistry* 40 (26), 4169–4194, 1997.
- Horti AG, Villemagne VL. The quest for Eldorado: Development of radioligands for in vivo imaging of nicotinic acetylcholine receptors in human brain. *Current Pharmaceutical Design* 12 (30), 3877–3900, 2006.
- Horti AG, Koren AO, Ravert HT, Musachio JL, Mathews WB, London ED, Dannals RF. Synthesis of a radiotracer for studying nicotinic acetylcholine receptors: 2-[ $^{18}\text{F}$ ]fluoro-3-(2(S)-azetidinylmethoxy)pyridine (2-[ $^{18}\text{F}$ ]A-85380). *Journal of Labelled Compounds & Radiopharmaceuticals* 41 (4), 309–318, 1998a.
- Horti AG, Scheffel U, Kimes AS, Musachio JL, Ravert HT, Mathews WB, Zhan Y, Finley PA, London ED, Dannals RF. Synthesis and evaluation of N-[11C]methylated analogues of epibatidine as tracers for positron emission tomographic studies of nicotinic acetylcholine receptors. *Journal of Medicinal Chemistry* 41 (22), 4199–4206, 1998b.
- Horti AG, Scheffel U, Koren AO, Ravert HT, Mathews WB, Musachio JL, Finley PA, London ED, Dannals RF. 2-[ $^{18}\text{F}$ ]fluoro-A-85380, an in vivo tracer for the nicotinic acetylcholine receptors. *Nuclear Medicine and Biology* 25 (7), 599–603, 1998c.
- Horti AG, Chefer SI, Mukhin AG, Koren AO, Gundisch D, Links JM, Kurian V, Dannals RF, London ED. 6-[ $^{18}\text{F}$ ]fluoro-A-85380, a novel radioligand for in vivo imaging of central nicotinic acetylcholine receptors. *Life Sciences* 67 (4), 463–469, 2000.
- Huang Y, Zhu Z, Xiao Y, Laruelle M. Epibatidine analogues as selective ligands for the alpha(x)beta2-containing subtypes of nicotinic acetylcholine receptors. *Bioorganic and Medicinal Chemistry Letters* 15 (19), 4385–4388, 2005.
- Kimes AS, Chefer SI, Matochik JA, Contoreggi CS, Vaupel DB, Stein EA, Mukhin AG. Quantification of nicotinic acetylcholine receptors in the human brain with PET: Bolus plus infusion administration of 2-[ $^{18}\text{F}$ ]F-A85380. *Neuroimage* 39 (2), 717–727, 2008.
- Kozikowski AP, Chellappan SK, Henderson D, Fulton R, Giboureaux N, Xiao Y, Wei ZL, Guilloteau D, Emond P, Dolle F, Kellar KJ, Kassiou M. Acetylenic pyridines for use in PET imaging of nicotinic receptors. *ChemMedChem* 2 (1), 54–57, 2006.
- Lin NH, Dong L, Bunnelle WH, Anderson DJ, Meyer MD. Synthesis and biological evaluation of pyridine-modified analogues of 3-(2-aminoethoxy)pyridine as novel nicotinic receptor ligands. *Bioorganic and Medicinal Chemistry Letters* 12 (22), 3321–3324, 2002.
- Lukas RJ, Changeux JP, Le Novere N, Albuquerque EX, Balfour DJ, Berg DK, Bertrand D, Chiappinelli VA, Clarke PB, Collins AC, Dani JA, Grady SR, Kellar KJ, Lindstrom JM, Marks MJ, Quik M, Taylor PW, Wonnacott S. International Union of Pharmacology. XX. Current status of the nomenclature for nicotinic acetylcholine receptors and their subunits. *Pharmacological Reviews* 51 (2), 397–401, 1999.
- Maziere M, Comar D, Marazano C, Berger G. Nicotine-11C: Synthesis and distribution kinetics in animals. *European Journal of Nuclear Medicine* 1 (4), 255–258, 1976.
- Mitkovski S, Villemagne VL, Novakovic KE, O'Keefe G, Tochon-Danguy H, Mulligan RS, Dickinson KL, Saudner T, Gregoire MC, Bottlaender M, Dolle F, Rowe CC. Simplified quantification of nicotinic receptors with 2-[ $^{18}\text{F}$ ]F-A-85380 PET. *Nuclear Medicine and Biology* 32 (6), 585–591, 2005.
- Molina PE, Ding YS, Carroll FI, Liang F, Volkow ND, Pappas N, Kuhar M, Abumrad N, Gatley SJ, Fowler JS. Fluoro-norchloroepibatidine: Preclinical assessment of acute toxicity. *Nuclear Medicine and Biology* 24 (8), 743–747, 1997.
- Mukhin AG, Kimes AS, Chefer SI, Matochik JA, Contoreggi CS, Horti AG, Vaupel BD, Pavlova O, Stein EA. Greater nicotinic acetylcholine receptor density in smokers compared to non-smokers: A PET imaging study with 2-[ $^{18}\text{F}$ ]F-A-85380. *Journal of Nuclear Medicine* 49, (1628–1635), 2008.
- Muzic Jr RF, Berridge MS, Friedland RP, Zhu N, Nelson AD. PET quantification of specific binding of carbon-11-nicotine in human brain. *Journal of Nuclear Medicine* 39 (12), 2048–2054, 1998.
- Ochoa EL, Lasalde-Dominicci J. Cognitive deficits in schizophrenia: Focus on neuronal nicotinic acetylcholine receptors and smoking. *Cellular and Molecular Neurobiology* 27 (5), 609–639, 2007.
- Paterson D, Nordberg A. Neuronal nicotinic receptors in the human brain. *Progress in Neurobiology* 61 (1), 75–111, 2000.
- Picard F, Bruel D, Servent D, Saba W, Fruchart-Gaillard C, Schollhorn-Peyronneau MA, Roumenov D, Brodtkorb E, Zuberi S, Gambardella A, Steinborn B, Hufnagel A, Valette H, Bottlaender M. Alteration of the in vivo nicotinic receptor density in ADNFLE patients: A PET study. *Brain* 129 (Pt 8), 2047–2060, 2006.
- Pichika R, Easwaramoorthy B, Collins D, Christian BT, Shi B, Narayanan TK, Potkin SG, Mukherjee J. Nicotinic alpha4beta2 receptor imaging agents: Part II. Synthesis and biological evaluation of 2-[ $^{18}\text{F}$ ]fluoro-3-[2-(S)-(pyrrolidinyl)methoxy]pyridine ( $^{18}\text{F}$ -nifene) in rodents and imaging by PET in nonhuman primate. *Nuclear Medicine and Biology* 33 (3), 295–304, 2006.
- Pimlott SL, Piggett M, Owens J, Greally E, Court JA, Jaros E, Perry RH, Perry EK, Wyper D. Nicotinic acetylcholine receptor distribution in Alzheimer's disease, dementia with Lewy bodies, Parkinson's disease, and vascular dementia: In vitro binding study using 5-[125I]-A-85380. *Neuropsychopharmacology* 29 (1), 108–116, 2004.
- Rahmim A, Zaidi H. PET versus SPECT: Strengths, limitations and challenges. *Nuclear Medicine Communications* 29 (3), 193–207, 2008.
- Roger G, Saba W, Valette H, Hinnen F, Coulon C, Ottaviani M, Bottlaender M, Dolle F. Synthesis and radiosynthesis of [ $^{18}\text{F}$ ]FPhEP, a novel alpha(4)beta(2)-selective, epibatidine-based antagonist for PET imaging of nicotinic acetylcholine receptors. *Bioorganic and Medicinal Chemistry* 14 (11), 3848–3858, 2006.
- Sabri O, Kendziorra K, Wolf H, Gertz HJ, Brust P. Acetylcholine receptors in dementia and mild cognitive impairment. *European Journal of Nuclear Medicine and Molecular Imaging* 35 (Suppl 1), S30–45, 2008.
- Scheffel U, Horti AG, Koren AO, Ravert HT, Banta JP, Finley PA, London ED, Dannals RF. 6-[ $^{18}\text{F}$ ]fluoro-A-85380: an in vivo tracer for the nicotinic acetylcholine receptor. *Nuclear Medicine and Biology* 27 (1), 51–56, 2000.
- Schmaljohann J, Minnerop M, Karwath P, Gundisch D, Falkai P, Gohlke S, Wullner U. Imaging of central nAChRs with 2-[ $^{18}\text{F}$ ]F-A85380: Optimized synthesis and in vitro evaluation in Alzheimer's disease. *Applied Radiation and Isotopes* 61 (6), 1235–1240, 2004.

- Sihver W, Fasth KJ, Ogren M, Lundqvist H, Bergstrom M, Watanabe Y, Langstrom B, Nordberg A. In vivo positron emission tomography studies on the novel nicotinic receptor agonist [ $^{11}\text{C}$ ]MPA compared with [ $^{11}\text{C}$ ]ABT-418 and (S)-(-)-[ $^{11}\text{C}$ ]nicotine in rhesus monkeys. *Nuclear Medicine and Biology* 26 (6), 633–640, 1999.
- Sihver W, Langstrom B, Nordberg A. Ligands for in vivo imaging of nicotinic receptor subtypes in Alzheimer brain. *Acta Neurologica Scandinavica. Supplementum* 176, 27–33, 2000a.
- Sihver W, Nordberg A, Langstrom B, Mukhin AG, Koren AO, Kimes AS, London ED. Development of ligands for in vivo imaging of cerebral nicotinic receptors. *Behavioural Brain Research* 113 (1–2), 143–157, 2000b.
- Sullivan JP, Donnelly-Roberts D, Briggs CA, Anderson DJ, Gopalakrishnan M, Piattoni-Kaplan M, Campbell JE, McKenna DG, Molinari E, Hettinger AM, Garvey DS, Wasicak JT, Holladay MW, Williams M, Arneric SP. A-85380 [3-(2(S)-azetidinylmethoxy)pyridine]: In vitro pharmacological properties of a novel, high affinity  $\alpha 4 \beta 2$  nicotinic acetylcholine receptor ligand. *Neuropharmacology* 35 (6), 725–734, 1996.
- Valette H, Bottlaender M, Doll F, Guenther I, Fuseau C, Coulon C, Ottaviani M, Crouzel C. Imaging central nicotinic acetylcholine receptors in baboons with [ $^{18}\text{F}$ ]fluoro-A-85380. *Journal of Nuclear Medicine* 40 (8), 1374–1380, 1999.
- Valette H, Dolle F, Saba W, Roger G, Hinnen F, Coulon C, Ottaviani M, Syrota A, Bottlaender M. [ $^{18}\text{F}$ ]FPhEP and [ $^{18}\text{F}$ ]F2PhEP, two new epibatidine-based radioligands: Evaluation for imaging nicotinic acetylcholine receptors in baboon brain. *Synapse* 61 (9), 764–770, 2007.
- Vaupel DB, Tella SR, Huso DL, Mukhin AG, Baum I, Wagner III VO, Horti AG, London ED, Koren AO, Kimes AS. Pharmacology, toxicology, and radiation dosimetry evaluation of [ $^{123}\text{I}$ ]5-I-A-85380, a radioligand for in vivo imaging of cerebral neuronal nicotinic acetylcholine receptors in humans. *Drug Development Research* 58 (2), 149–168, 2003.
- Vaupel DB, Tella SR, Huso DL, Wagner 3rd VO, Mukhin AG, Chefer SI, Horti AG, London ED, Koren AO, Kimes AS. Pharmacological and toxicological evaluation of 2-fluoro-3-(2(S)-azetidinylmethoxy)pyridine (2-F-A-85380), a ligand for imaging cerebral nicotinic acetylcholine receptors with positron emission tomography. *Journal of Pharmacology and Experimental Therapeutics* 312 (1), 355–365, 2005.
- Villemagne VL, Musachio JL, Scheffel U. Nicotine and related compounds as PET and SPECT ligands. In: Arneric, SP, Brioni, JD (Eds.), *Neuronal Nicotinic Receptors, Pharmacology and Therapeutic Opportunities*. Johns Wiley & Sons, New York, pp. 235–250, 1999.
- Volkow ND, Ding YS, Fowler JS, Gatley SJ. Imaging brain cholinergic activity with positron emission tomography: Its role in the evaluation of cholinergic treatments in Alzheimer's dementia. *Biological Psychiatry* 49 (3), 211–220, 2001.
- Watabe H, Endres CJ, Breier A, Schmall B, Eckelman WC, Carson RE. Measurement of dopamine release with continuous infusion of [ $^{11}\text{C}$ ]raclopride: optimization and signal-to-noise considerations. *Journal of Nuclear Medicine* 41 (3), 522–530, 2000.
- Wei ZL, Xiao Y, Yuan H, Baydyuk M, Petukhov PA, Musachio JL, Kellar KJ, Kozikowski AP. Novel pyridyl ring C5 substituted analogues of epibatidine and 3-(1-Methyl-2(S)-pyrrolidinylmethoxy)pyridine (A-84543) as highly selective agents for neuronal nicotinic acetylcholine receptors containing  $\beta 2$  subunits. *Journal of Medicinal Chemistry* 48 (6), 1721–1724, 2005.
- Zhang Y, Horti AG. Synthesis of 6-chloro-3-((2-(S)-azetidinyl)methoxy)-5-(2-[ $^{18}\text{F}$ ]fluoropyridin-4-yl)pyridine ([ $^{18}\text{F}$ ]NIDA 522131), a novel potential radioligand for studying extrathalamic nicotinic acetylcholine receptors by PET. *Journal of Labelled Compounds & Radiopharmaceuticals* 47 (13), 947–952, 2004.
- Zhang Y, Pavlova OA, Chefer SI, Hall AW, Kurian V, Brown LL, Kimes AS, Mukhin AG, Horti AG. 5-Substituted Derivatives of 6-Halogeno-3-((2-(S)-azetidinyl)methoxy)pyridine and 6-Halogeno-3-((2-(S)-pyrrolidinyl)methoxy)pyridine with low picomolar affinity for  $\alpha 4 \beta 2$  nicotinic acetylcholine receptor and wide range of lipophilicity: Potential probes for imaging with positron emission tomography. *Journal of Medicinal Chemistry* 47 (10), 2453–2465, 2004.